Original Article

MOLECULAR METABOLISM

Glycaemia and body weight are regulated by sodium-glucose cotransporter 1 (SGLT1) expression via *O*-GlcNAcylation in the intestine

Kimihiro Nishimura [1], Yukihiro Fujita [1,*], Shogo Ida [1], Tsuyoshi Yanagimachi [1], Natsuko Ohashi [1], Kiyoto Nishi [2], Atsushi Nishida [1], Yasumasa Iwasaki [3], Katsutaro Morino [1,4], Satoshi Ugi [1], Eiichiro Nishi [2], Akira Andoh [1], Hiroshi Maegawa [1]

ABSTRACT

Objective: The intestine is an important organ for nutrient metabolism via absorption and endocrine systems. Nutrients regulate *O*-GlcNAcylation, a post-translational modification of various proteins by *O*-GlcNAc transferase (OGT). We have previously shown that general OGT knockout induced severe weight loss and hypoglycaemia in mice, but little is known about how *O*-GlcNAcylation in the intestine modulates nutrient metabolism, especially glucose metabolism, through absorption. We aimed to reveal the roles of *O*-GlcNAcylation in glucose absorption by the small intestine and elucidate the mechanism by which *O*-GlcNAcylation regulates sodium-glucose cotransporter 1 (SGLT1) expression.

Methods: First, we fasted normal mice and examined the changes in glucose transporters and *O*-GlcNAcylation in the intestine. Then, we generated two lines of small intestine-specific OGT-deficient mice (congenital: *Ogt*-VKO, tamoxifen-inducible: *Ogt*-iVKO) and observed the changes in body weight and in glucose and lipid metabolism. Finally, we investigated *Sglt1* gene regulation by *O*-GlcNAcylation using enteroendocrine STC-1 cells.

Results: Fasting decreased *O*-GlcNAcylation in the intestinal epithelium of normal mice. The *Ogt*-VKO mice showed significantly lower non-fasted blood glucose levels and were underweight compared with litter matched controls. Glycaemic excursion in the *Ogt*-VKO mice was significantly lower during the oral glucose tolerance test but comparable during the intraperitoneal glucose tolerance test. Furthermore, the *Ogt*-VKO mice exhibited lower *Sglt1* expression in the small intestine compared with the control mice. We obtained similar results using the *Ogt*-iVKO mice only after tamoxifen administration. The oral D-xylose administration test revealed that the intestinal sugar absorption was diminished in the *Ogt*-iVKO mice and that GLP-1 secretion did not sufficiently increase after glucose gavage in the *Ogt*-iVKO mice. When using STC-1 cells, *O*-GlcNAcylation increased *Sglt1* mRNA via a PKA/CREB-dependent pathway.

Conclusion: Collectively, loss of *O*-GlcNAcylation in the intestine reduced glucose absorption via suppression of SGLT1 expression; this may lead to new treatments for malabsorption, obesity and diabetes.

Keywords Intestine; *O*-GlcNAcylation; SGLT1; Glucose absorption; GLP-1

1. INTRODUCTION

The intestine is an important organ for digestion, absorption, immunity and endocrine systems. Intestinal epithelial cells line the inner surface of the small intestine and consist of four different cell types: enterocytes (intestinal absorptive cells), Paneth cells, goblets cells and enteroendocrine cells [1]. The small intestine digests nutrients such as carbohydrates, proteins and fats and absorbs them from the apical sites of enterocytes into the capillaries and the lymph vessels via either diffusion or active transport [2]. More than 20 hormones are released from enteroendocrine cells, which are involved in the regulation of digestive juice secretion, gut motility, appetite and nutrient metabolism. GLP-1 and GIP are incretins involved in the glucose-dependent insulin secretion from pancreatic beta cells. GLP-1 also regulates food intake and suppresses glucagon secretion from pancreatic alpha cells, and GIP is involved in functions such as bone and fat metabolism [3,4]. With the advent of new classes of glucose-lowering drugs for diabetes, various organs have been shown to be involved in the pathogenesis of hyperglycaemia, including the gastrointestinal tract via diminished actions of incretins [5,6].

Glucose, one of the body's most important energy sources, is absorbed by the active sugar transporter, SGLT1, at the brush border of enterocytes; it is then extruded to the basolateral sites by the facilitated glucose transporter, GLUT2 [7]. A missense mutation in the *SGLT1* gene in humans causes the inherited metabolic disorder of glucose-galactose malabsorption with symptoms that include watery and/or

[1]Department of Medicine, Shiga University of Medical Science, Shiga 520-2192, Japan [2]Department of Pharmacology, Shiga University of Medical Science, Shiga 520-2192, Japan [3]Department of Clinical Nutrition, Faculty of Health Science, Suzuka University of Medical Science, Mie 510-029, Japan [4]Institutional Research Office, Shiga University of Medical Science, Shiga 520-2192, Japan

*Corresponding author. E-mail: fujita@belle.shiga-med.ac.jp (Y. Fujita).

Received December 2, 2021 • Revision received February 10, 2022 • Accepted February 10, 2022 • Available online 19 February 2022

https://doi.org/10.1016/j.molmet.2022.101458

Abbreviations

CREB	cAMP response element binding protein
EE	energy expenditure
GIP	glucose-dependent insulinotropic polypeptide
GLP-1	glucagon-like peptide-1
GLUT	glucose transporter
IPGTT	intraperitoneal glucose tolerance test
O-GlcNAcylation	*O*-linked N-acetylglucosaminylation
OGA	*O*-GlcNAcase
OGT	*O*-GlcNAc transferase
OGTT	oral glucose tolerance test
OOTT	olive oil tolerance test
OSMI1	αR-[[(1,2-dihydro-2-oxo-6-quinolinyl)sulfonyl]amino]-N-(2-furanylmethyl)-2-methoxy-N-(2-thienylmethyl)-benzeneacetamide
PKA	protein kinase A
RQ	respiratory quotient
SGLT1	sodium-glucose cotransporter 1

acidic diarrhoea by non-absorbed glucose, galactose and sodium [8,9]. SGLT1 is also expressed in the apical membrane of incretin-secreting K cells and L cells and functions as a glucose sensor. Incretin release is enhanced mainly after sugar and lipid intake. *Sglt1*-deficient mice lack glucose-stimulated incretin secretion but sustain lipid-stimulated incretin release [10].

Glucose in the cells enters the hexosamine biosynthetic pathway and is converted partly into uridine diphosphate N-acetylglucosamine (UDP-GlcNAc). *O*-GlcNAcylation is a post-translational modification in which UDP-GlcNAc is added to the serine/threonine residues of target proteins and modulates activation or inactivation of various proteins and genes' expression. Amino acids and fatty acid metabolites are involved in *O*-GlcNAcylation, in addition to glucose metabolites, and only two key enzymes regulate *O*-GlcNAcylation: the enhancer OGT and the suppressor OGA [11,12]. Several reports have indicated that *O*-GlcNAcylation was enhanced in diabetes mellitus, resulting in glucotoxicity, enhanced insulin resistance, impaired insulin secretion and diabetic complications [13–17].

We have previously generated mice with a tamoxifen-induced *OGT* knockout in the entire body and reported that the general OGT depletion induced severe weight loss and hypoglycaemia, eventually resulting in death. Additionally, mice with pancreatic beta cell-specific OGT depletion manifested insulin hypersecretion in the early stage, followed by beta cell apoptosis with decreased insulin secretion in the late stage [18]. However, little is known about how *O*-GlcNAcylation in the intestine modulates nutrient metabolism, especially glucose metabolism, through absorption.

We attempted to elucidate the physiological and pathophysiological roles of *O*-GlcNAcylation in the small intestine, which plays important roles in the absorption of nutrients and the regulation of systemic metabolism. To this end, we generated two lines of small intestine-specific OGT-deficient mice and observed the changes in body weight and glucose and lipid metabolism, then investigated the roles of *O*-GlcNAcylation *in vivo* and *in vitro*.

2. METHODS

2.1. Ethics

All animal experiments were conducted in accordance with the guidelines of the Research Center for Animal Life Science (RCALS), and all animal experimental protocols were approved by the Safety Committee for Genetic Recombination Experiments and RCALS, Shiga University of Medical Science (Approval numbers #26-7, #29-32, #30-37). All animal handling and experimentation were conducted according to the guidelines of RCALS at Shiga University of Medical Science.

2.2. Animal experiments

For fasting experiments, C57BL/6J male mice (Nihon Clea, Tokyo, Japan) were fasted for 24 h with free access to water. Intestinal epithelial-specific *Ogt*-deficient mice (*Ogt*-VKO), tamoxifen-inducible intestinal epithelial-specific *Ogt*-deficient mice (*Ogt*-iVKO) and whole-body tamoxifen-inducible *Ogt*-deficient mice (*Ogt*-iKO) were generated using the Cre-LoxP system by mating *Ogt*-flox (*Ogt* flox/flox) female mice (Jackson Laboratory, Bar Harbor, ME, USA). Further details are described in the Supplemental methods and figures (SFigures 1A, 3A, 9A).

All animals were housed in a facility kept at 23 °C and a 12-h light/dark cycle. Unless otherwise noted, mice were kept in groups and had free access to water and standard solid chow. The experiments used only male mice (4–22 weeks).

2.3. Oral glucose tolerance test (OGTT), intraperitoneal glucose tolerance test (IPGTT), olive oil tolerance test (OOTT) and i.v. lipid tolerance test

The mice were fasted for 16–18 h before tests were performed. We administered by gavage a 20% w/v glucose solution (1 g/kg body weight) or injected the solution intraperitoneally, then measured blood glucose levels and plasma insulin levels as described in the Supplemental Methods.

In the OOTT, we administered by gavage olive oil (olive oil: 5 ml/kg body weight) and collected blood samples from the tail vein at 1, 2, 4, 6 and 8 h after administration. The i.v. lipid tolerance test was performed after 16–18 h of fasting, with i.v. injection of a lipid emulsion (Intralipos® Injection 20%: 7.5 ml/kg body weight; Otsuka Pharmaceutical Factory, Inc., Tokushima, Japan) via the middle of the tail vein. Blood samples were collected from the end of the tail vein at 1, 3, 6, 10 and 15 min after administration [19]. Triglyceride levels were measured by an enzymatic colourimetric method (290-63701; FUJIFILM Wako Pure Chemical Corporation, Osaka, Japan). For assessment of faecal triglyceride content, we extracted triglyceride from the faecal per the method of Bligh and Dyer [20] and measured as described above.

2.4. Respiratory and metabolic analysis

The *Ogt*-flox and the *Ogt*-VKO mice were individually housed in chambers at 23 ± 1 °C under a 12-h light (08:00–20:00)/12-h dark (20:00–8:00) cycle for 3 days. Then, respiratory and metabolic parameters were measured for 2 days. Gas analysis was performed every 10 min using indirect calorimetry (Comprehensive Lab Animal Monitoring System: Oxymax/CLAMS, Columbus Instruments, TX, US). We measured respiratory quotient (RQ), locomotive activities (Xtot) and energy expenditure (EE).

2.5. Oral D-xylose administration test

We administered D-xylose solution (1 g/kg body weight) by gavage after 4 h fasting and collected blood samples from the tail vein at 0, 30, 60 and 120 min after administration [21,22]. After centrifuge, we assayed serum D-xylose levels by commercial ELISA kits (#6601; Condrex, Bucharest, Romania).

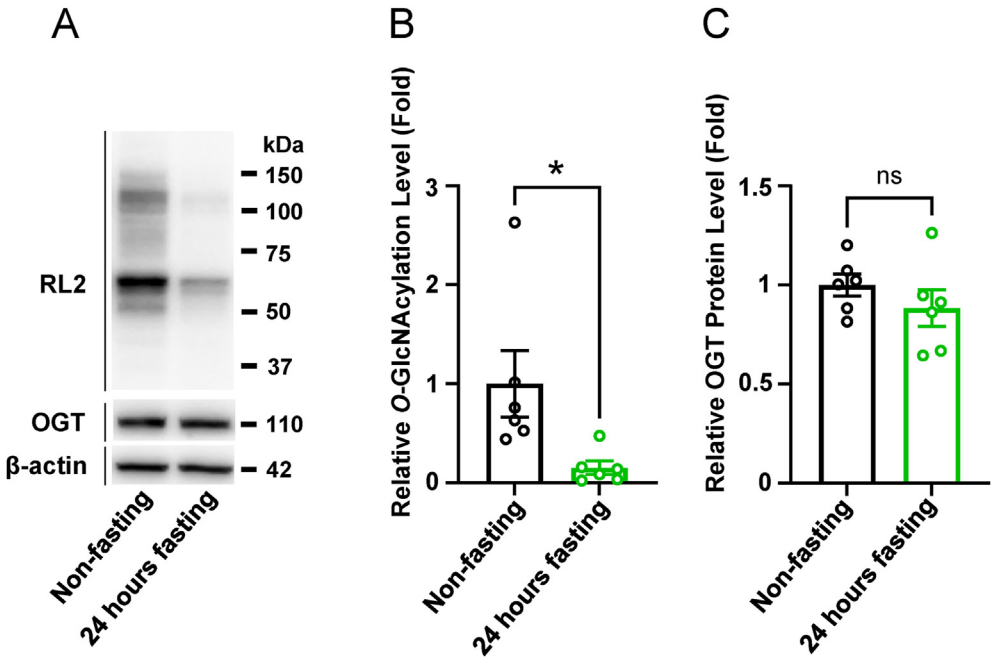

Figure 1: Fasting reduced *O*-GlcNAcylation in the intestinal epithelium. (A) Representative western blot analysis of *O*-GlcNAcylation (RL2) and OGT levels in the intestinal epithelium. Quantification of RL2 (B) and OGT (C) levels in the intestinal epithelium (n = 6 in each group). Data are presented as mean ± SEM. $*p < 0.05$, $**p < 0.01$.

2.6. Glucose-induced or lipid-induced incretin secretion

We examined glucose-induced or lipid-induced incretin secretion in mice as described in the Supplemental Methods and in a previous report [10]. Total GIP and total GLP-1 were assayed by commercial ELISA kits (GIP: EZRMGIP-55K, GLP-1: EZGLP1T-36K; Millipore, Burlington, MA, USA).

2.7. Histological analysis and western blot analysis

The antibodies and methods used are described in the Supplemental Methods.

2.8. Cell experiments

Professor Douglas Hanahan kindly provided Enteroendocrine STC-1 cells. The cells were grown in 25 mmol/l glucose DMEM with 10% FCS and 1% Pen Strep in 5% CO_2 at 37 °C. We cultured the cells to around 70–90% confluency for experiments. We examined the effects of *O*-GlcNAcylation and intrinsic cAMP activation on the regulation of *Sglt*1 gene expression in STC-1 cells. For *O*-GlcNAcylation, cells were incubated for 3 days with 10 mmol/l D-glucosamine hydrochloride (11712-24; Nacalai Tesque Inc., Kyoto, Japan). For suppression of *O*-GlcNAcylation, the OGT inhibitor OSM1 (SML1621; Sigma-Aldrich, St. Louis, MO, USA) was added to the medium at 50 μmol/l on the last day of D-glucosamine treatment. For PKA inhibition or CREB inhibition, we incubated STC-1 cells in the medium with H89 at 10 μmol/l (10010556; Cayman Chemical, Ann Arbor, MI, USA) or 666-15 at 100 nmol/l (538341; Sigma-Aldrich, St. Louis, MO, USA) for 24 h.

2.9. Total RNA extraction and qRT-PCR analysis

We performed total RNA extraction, cDNA synthesis and qRT-PCR analysis as described in the Supplemental Methods. Primer sequences are listed in the Supplemental Materials (Stable 1).

2.10. Statistical analysis

Data are expressed as mean ± SEM. Statistical analysis was performed using the unpaired Student's *t* test, one-way ANOVA followed by Tukey *post hoc* test, two-way repeated ANOVA followed by the Sidak *post hoc* test or analysis of covariance (ANCOVA). Data were analysed using commercial software (Generic analysis, Prism 9; GraphPad, San Diego, CA, USA. ANCOVA, SPSS version 25; SPSS Inc., Armonk, NY, USA). A value of $p < 0.05$ was considered as significant.

3. RESULTS

3.1. Fasting reduces *O*-GlcNAcylation in the intestinal epithelium

It is not well documented whether *O*-GlcNAcylation increases or decreases upon physiological changes after feeding in the intestinal epithelium, although *O*-GlcNAcylation has previously been shown to function as a nutrient sensor in other organs [23].

Thus, we compared 24-h-fasted mice with non-fasting control mice to examine whether *O*-GlcNAcylation in intestinal epithelial cells was modified by starvation. *O*-GlcNAcylation in the small intestine of the 24-h-fasted mice was about a fifth of that in the non-fasting control mice as assessed by the expression of *O*-linked N-acetylglucosamine, detected with RL2 antibody, though the OGT protein levels were comparable (Figure 1A–C). Thus, fasting decreased the expression of *O*-GlcNAcylation level in the intestinal epithelium.

3.2. Intestine-specific OGT depletion reduces glycaemia and body weight in the mice

To further explore the roles of *O*-GlcNAcylation in the intestinal epithelium, we generated mice with an intestinal epithelium-specific knockout of *Ogt* gene (*Ogt*-VKO) by mating female *Ogt* (flox/flox) mice with male villin1-Cre transgenic mice (SFigure 1A). First, we confirmed that *O*-GlcNAcylation was diminished in the small intestine of the *Ogt*-VKO mice by showing the lack of expression of *O*-linked N-acetylglucosamine in the intestinal epithelium through western blotting and immunohistochemistry with RL2 antibody (Figure 2A,B), and *Ogt* gene expression was reduced in the intestinal mucosa of the *Ogt*-VKO mice (Figure 2C). Furthermore, the *Ogt*-VKO mice had significantly lower non-fasted blood glucose levels than the litter-matched controls

(at 4 weeks; 7.7 ± 0.4 vs. 5.1 ± 0.2 mmol/L, $p < 0.05$; Figure 2D). The glycaemia in the *Ogt*-VKO mice remained significantly lower than in the control mice during the entire observation period. Compared with the control mice, the *Ogt*-VKO mice were also significantly underweight at weaning (4 weeks; 22.3 ± 0.3 vs. 15.9 ± 0.4 g, $p < 0.05$), and their subsequent body weight gain was notably reduced during their growth (Figure 2E,F).

3.3. Glucose absorption from the small intestine may be decreased in the *Ogt*-VKO mice

We performed OGTT, IPGTT and OOTT to determine the effect of *O*-GlcNAcylation on intestinal nutrient absorption. The *Ogt*-VKO mice showed significantly lower glucose excursion along with reduced insulin release in the OGTT compared with the control mice (Figure 3A–C). However, the changes in glycaemia and insulin levels were comparable during the IPGTT between the *Ogt*-VKO and the control mice (Figure 3D–F). We also observed comparable insulin sensitivity between the two groups, which we assessed with the insulin tolerance test (SFigure 1B). Contrary to the oral glucose load, the *Ogt*-VKO mice showed significantly higher triglyceride levels 2 h after oral olive oil gavage compared with the control mice (Figure 3G,H), but the *Ogt*-VKO mice showed lower triglyceride levels after i.v. injection of intralipos compared with the control mice (Figure 3I).

We expected that the *Ogt*-VKO mice would use less glucose and more lipids because of the limited glucose absorption from the intestine. We measured and compared the faecal lipid content to assess if the lipid absorption was enhanced in the *Ogt*-VKO mice. The faecal lipid contents from the *Ogt*-VKO mice showed approximately one-third of that of the control mice, suggesting the *Ogt*-VKO might absorb more lipids from the gut (Figure 4I).

Next, we performed respiratory and metabolic analyses. In the *Ogt*-VKO mice, the RQ significantly decreased between the dawn and the early light period compared with the control mice, suggesting lipid metabolism was enhanced during the period (Figure 4A,B). The

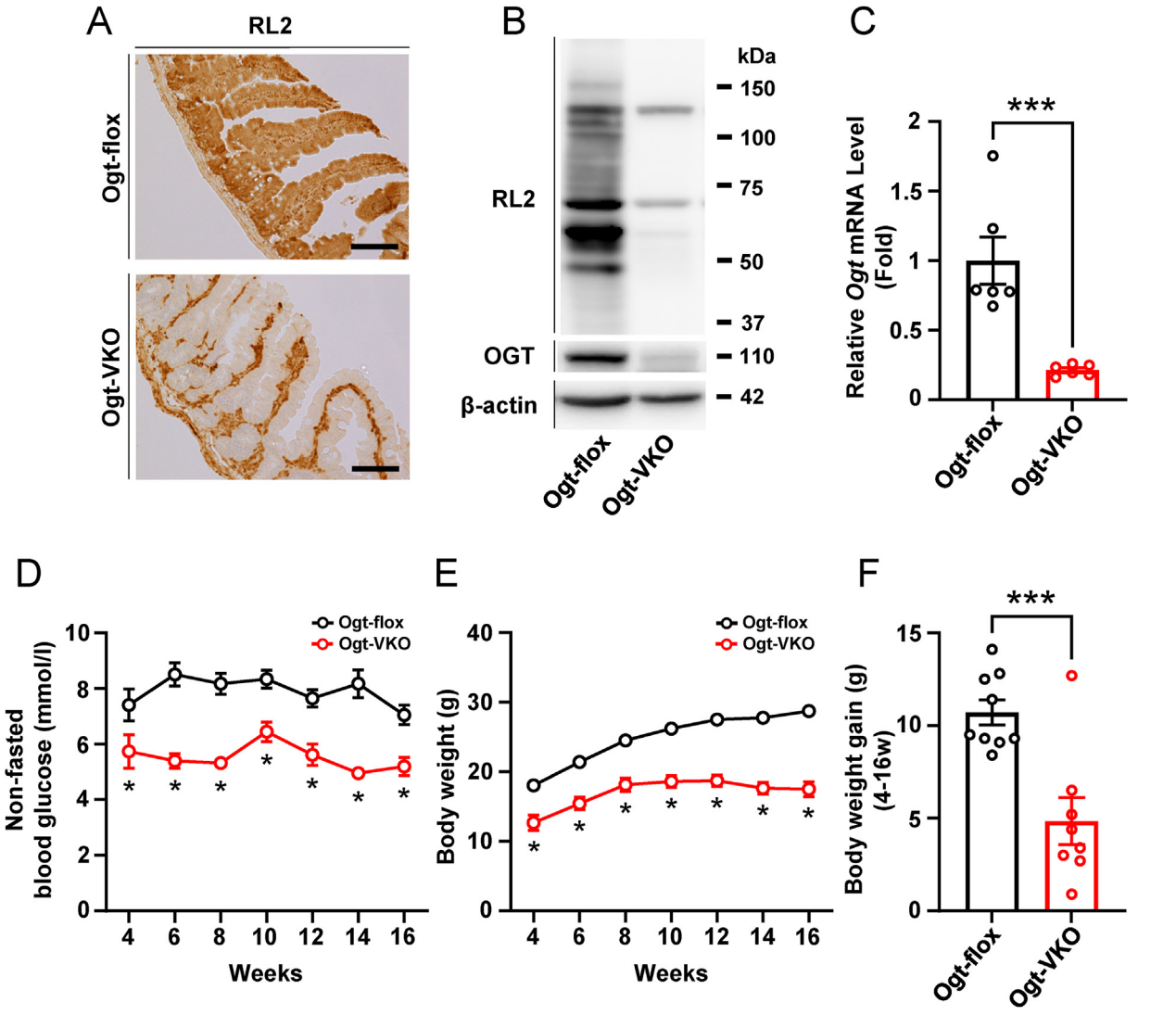

Figure 2: Intestine-specific OGT depletion reduced glycaemia and body weight in the mice. (A) Immunohistochemical analysis of *O*-GlcNAcylation in the intestinal epithelium using anti-*O*-GlcNAc (RL2) antibodies (scale bars, 100 μm). (B) Representative western blot analysis of *O*-GlcNAcylation (RL2) and OGT levels in the intestinal epithelium. (C) Quantification of *Ogt* gene expression in the intestinal epithelium (n = 6 in each group). (D) Body weight of the *O*gt-VKO and the control mice following weaning (n = 9 for the *O*gt-flox and n = 8 for the *Ogt*-VKO). (E) Blood glucose levels of the *Ogt*-VKO and the control mice following weaning (n = 9 for the *Ogt*-flox and n = 8 for the *Ogt*-VKO). (F) Body weight gain of the *Ogt*-VKO and the control mice from 4 to 16 weeks. Data are presented as means ± SEM. $*p < 0.05$, $***p < 0.001$.

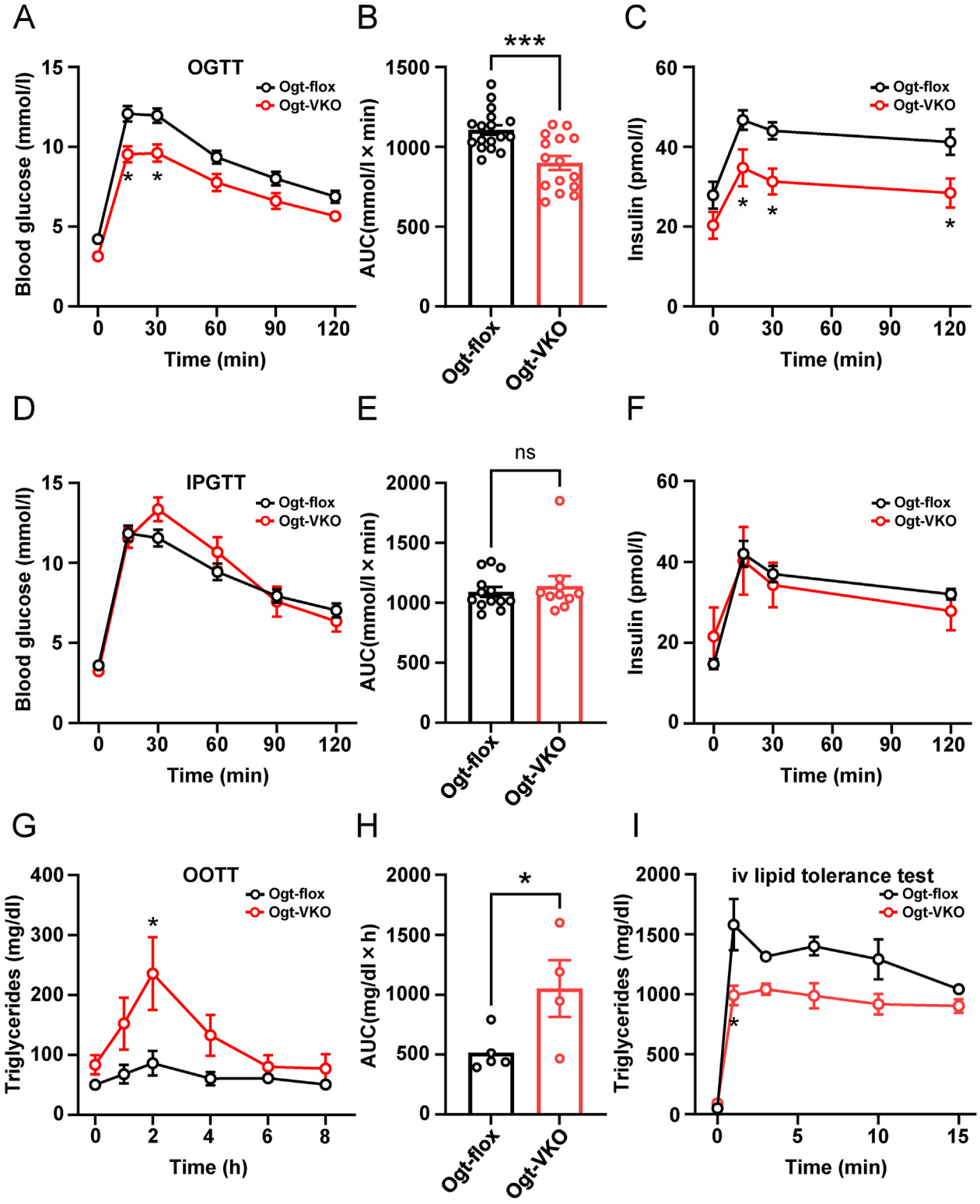

Figure 3: Glucose absorption from the small intestine was decreased in the *Ogt*-VKO mice. (A, B) Glycaemia and AUC of the *Ogt*-VKO and the control mice during the OGTT (n = 17 for the *Ogt*-flox and n = 15 for the *Ogt*-VKO). (C) Insulin secretion of the *Ogt*-VKO and the control mice (n = 9 for the *Ogt*-flox and n = 8 for the *Ogt*-VKO) during the OGTT. (D, E) Glycaemia and AUC of the *Ogt*-VKO and the control mice during the IPGTT (n = 13 for the *Ogt*-flox and n = 10 for the *Ogt*-VKO). (F) Insulin secretion of the *Ogt*-VKO and the control mice during the IPGTT (n = 10 for the *Ogt*-flox and n = 9 for the *Ogt*-VKO). (G, H) Triglyceride concentrations and AUC of the *Ogt*-VKO and the control mice during the OOTT (n = 5 for the *Ogt*-flox and n = 4 for the *Ogt*-VKO). (I) Triglyceride concentrations and AUC of the *Ogt*-VKO and the control mice during the i.v. intralipos tolerance test (n = 4 for the *Ogt*-flox and n = 3 for the *Ogt*-VKO). Data are presented as mean ± SEM. $^*p < 0.05$. AUC, area under the curve.

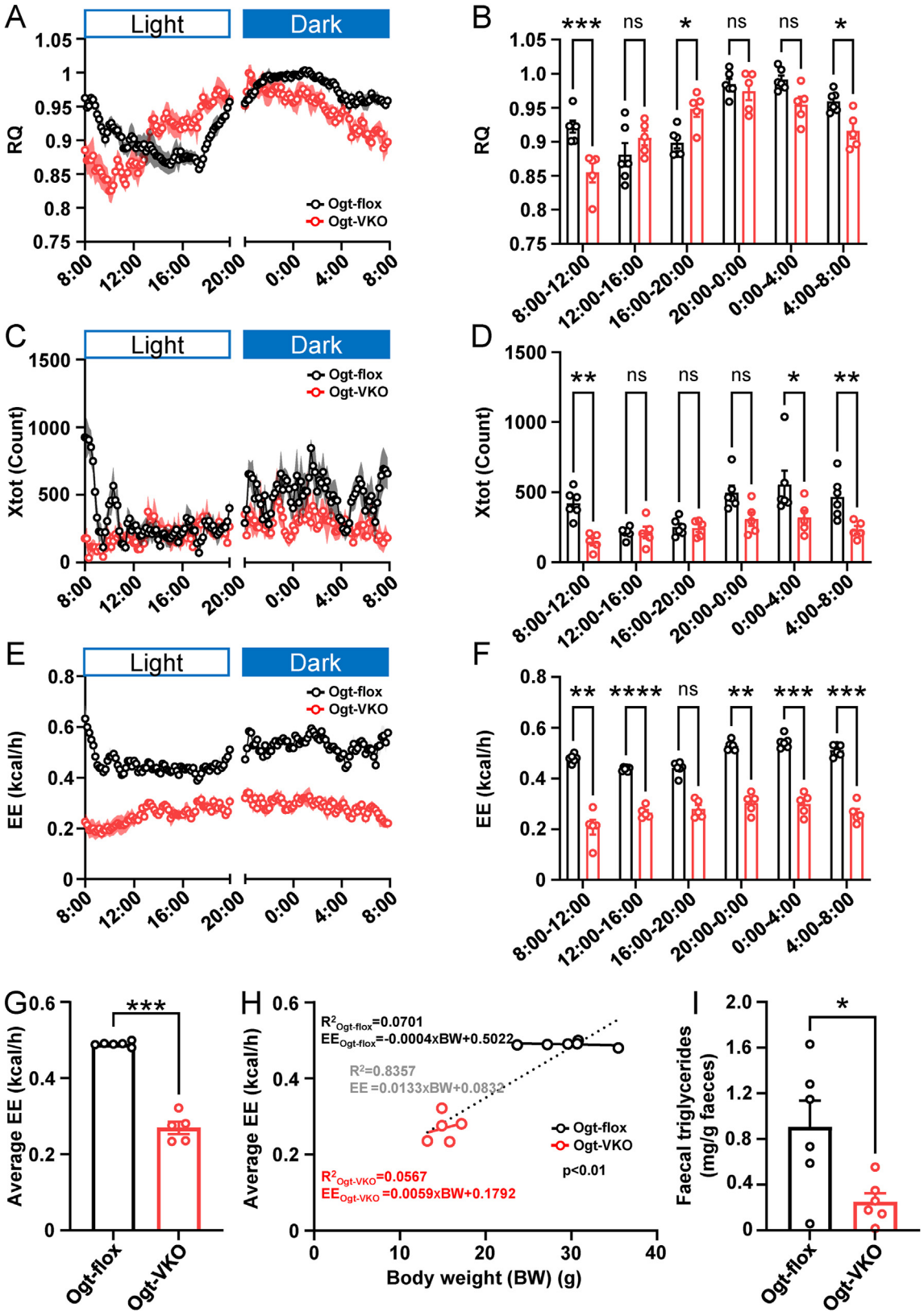

Figure 4: Faecal triglyceride content, respiratory quotient (RQ), voluntary activity (Xtot) and energy expenditure (EE). (A, B) RQ of the *Ogt*-VKO and the control mice (n = 6 for the *Ogt*-flox and n = 5 for the *Ogt*-VKO). (C, D) Voluntary activity (Xtot) of the *Ogt*-VKO and the control mice (n = 6 for the *Ogt*-flox and n = 5 for the *Ogt*-VKO). (E, F, G) Energy expenditure (EE) of the *Ogt*-VKO and the control mice (n = 6 for the *Ogt*-flox and n = 5 for the *Ogt*-VKO, dF = 1) (H) Generalized linear model of the *Ogt*-VKO and the control mice (n = 6 for the *Ogt*-flox and n = 5 for the *Ogt*-VKO, dF = 1). (I) Faecal triglyceride of the *Ogt*-VKO and the control mice (n = 6 in each group). Data are presented as mean ± SEM. $^*p < 0.05$, $^{**}p < 0.01$, $^{***}p < 0.001$. (Two-way ANOVA except for EE. ANCOVA for EE).

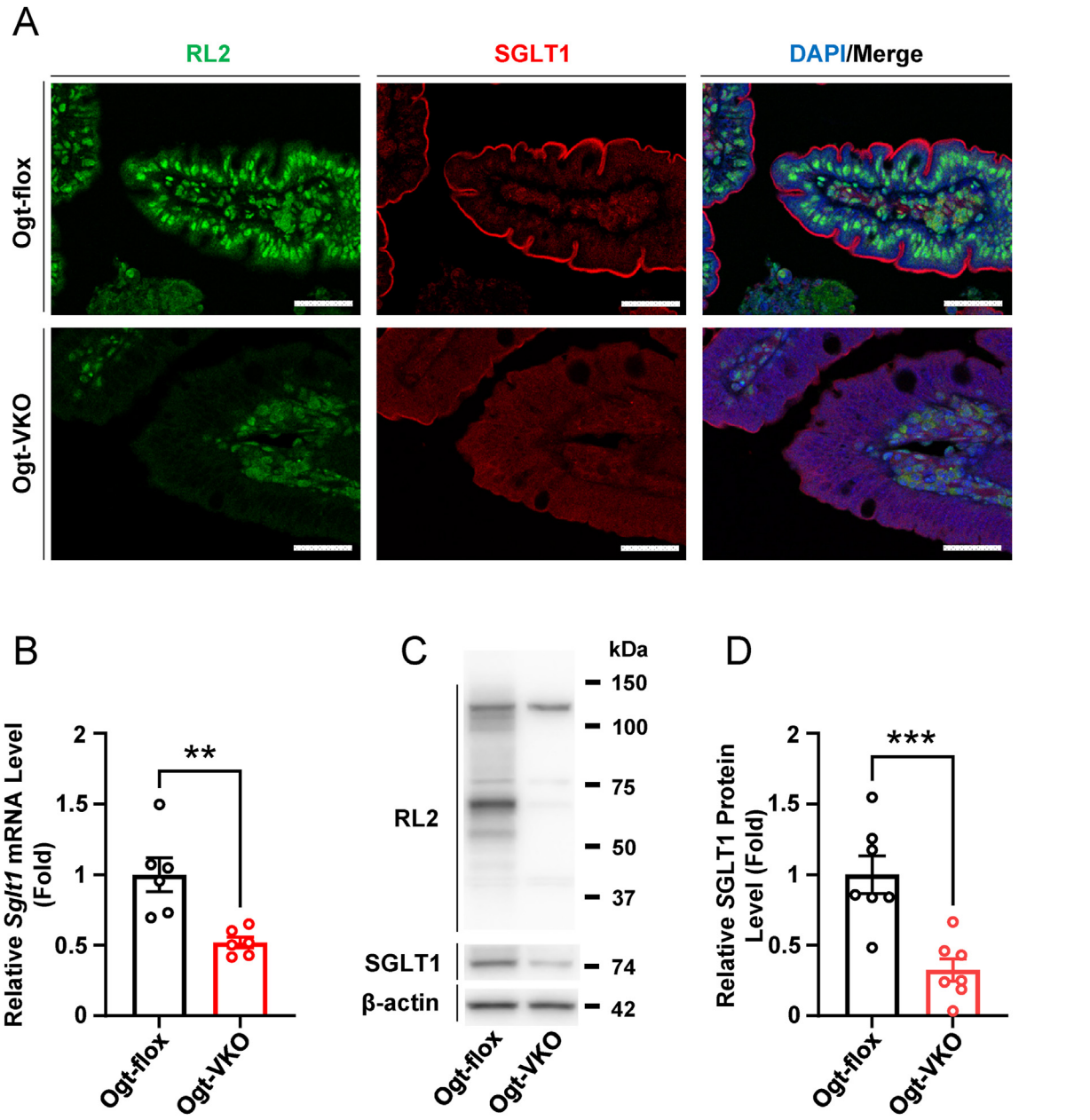

Figure 5: The *Ogt*-VKO mice exhibited lower expression of SGLT1 in the small intestine. (A) Intestinal epithelium sections were stained with RL2 (green), SGLT1 (red) and DAPI (blue); representative intestine epithelium images are shown (scale bars, 25 μm). (B) Quantification of *Sglt1* gene expression in the intestinal epithelium (n = 6 in each group). (C) Representative western blot analysis of SGLT1 levels in the intestinal epithelium. (D) Quantification of SGLT1 levels in the intestinal epithelium (n = 7 in each group). Data are presented as mean ± SEM. $^{**}p < 0.01$, $^{***}p < 0.001$.

locomotive activity (Xtot) of the control mice fluctuated, but that of the *Ogt*-VKO mice was stable and low during the mid-dark phase and the early light period (Figure 4C,D). Energy expenditure in the *Ogt*-VKO mice was lower for nearly the duration of the day than that in the control mice, with statistical significance by ANCOVA analysis in setting body weight as a confounding factor (n = 6 for the *Ogt*-flox and n = 5 for the *Ogt*-VKO, dF = 1, $p < 0.001$) (Figure 4E–G). We also plotted the individual average EE values and respective body weight of each mouse, indicating that the genetic manipulation was driving differences in EE and that body weight was not responsible for the differences since each slope was variable by the mouse genetics (Figure 4H).

These results suggest that glucose absorption may be diminished from the small intestine of the *Ogt*-VKO mice and that the *Ogt*-VKO mice could shift from glucose to lipid metabolism.

3.4. The *Ogt*-VKO mice exhibit lower expression of SGLT1 in the small intestine without atrophy and inflammation

In the control mice, strong SGLT1 expression was observed along the brush border membranes of the intestinal villi concomitantly with the expression of *O*-linked N-acetylglucosamine in the nucleus and the cytosol, which was detected with RL2 antibody. However, in the *Ogt*-VKO mice, SGLT1 expression was scarce, with almost no *O*-GlcNAcylation in the intestinal epithelium (Figure 5A). We also observed that the *Sglt1* gene

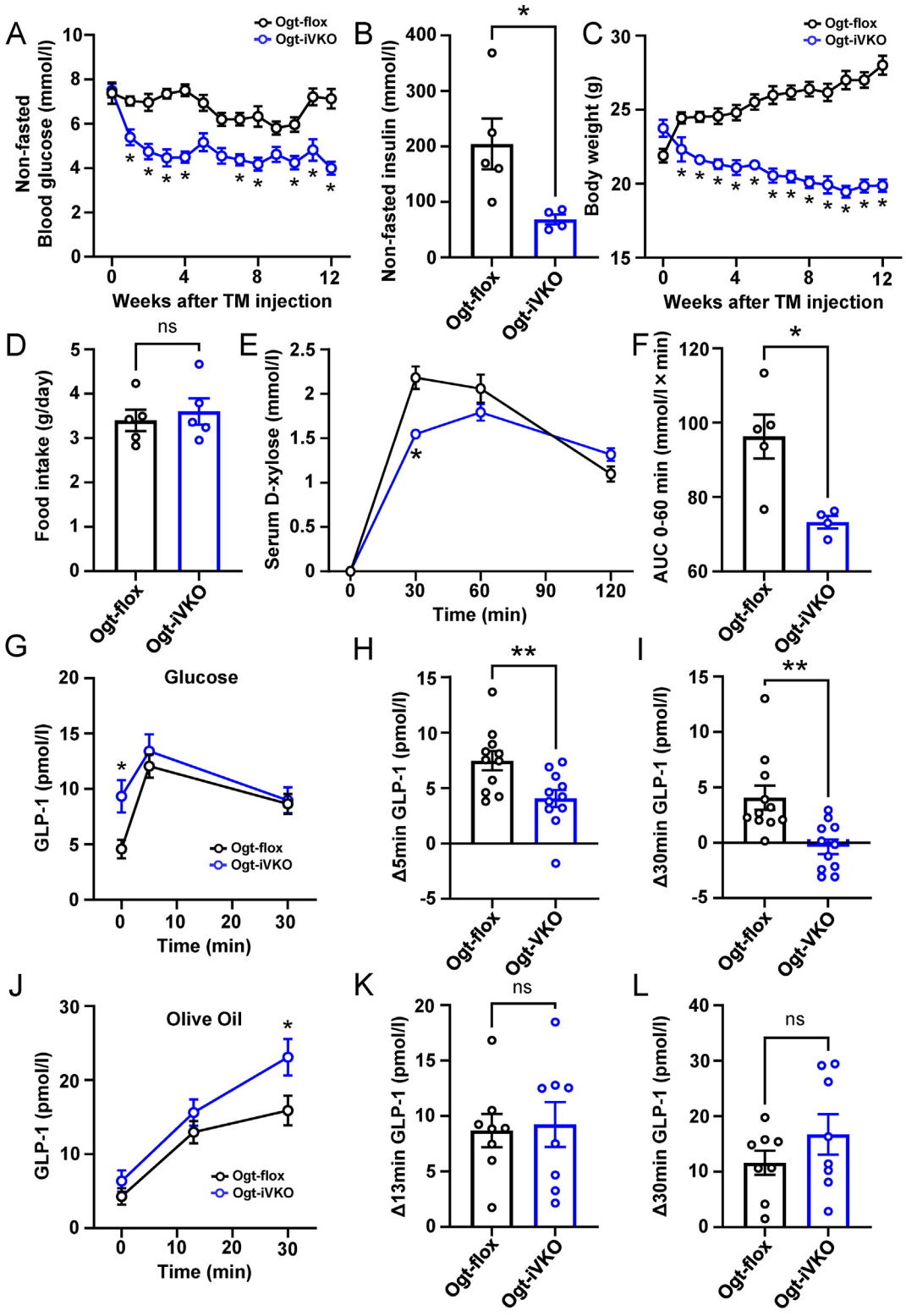

Figure 6: Induced small intestine-specific depletion of OGT decreased body weight and glycaemia and glucose-dependent GLP-1 secretion was blocked in the *Ogt*-iVKO mice. (A) Body weight of the *Ogt*-iVKO and the control mice following TM injection (n = 8 for the *Ogt*-flox and n = 7 for the *Ogt*-iVKO). (B) Non-fasted insulin secretion of the *Ogt*-VKO and the control mice (n = 5 for the *Ogt*-flox and n = 4 for the *Ogt*-iVKO). (C) Blood glucose levels of the *Ogt*-iVKO and the control mice following TM injection (n = 8 for the *Ogt*-flox and n = 7 for the *Ogt*-iVKO). (D) Food intake of the *Ogt*-iVKO and the control mice (n = 5 for the *Ogt*-flox and n = 5 for the *Ogt*-iVKO). (E, F) Serum D-xylose concentrations and AUC (up to 60 min) during the oral D-xylose administration test of the *Ogt*-iVKO and the control mice (n = 5 for the *Ogt*-flox and n = 4 for the *Ogt*-iVKO). (G) GLP-1 concentrations in the *Ogt*-iVKO and the control mice during the OGTT (n = 11 in each group). (H, I) ΔGLP-1 concentrations in the *Ogt*-iVKO and the control mice at 5 and 30 min after glucose gavage (n = 11 in each group). (J) GLP-1 concentrations in the *Ogt*-iVKO and the control mice during the OOTT (n = 8 in each group). (K, L) ΔGLP-1 concentrations in the *Ogt*-iVKO and the control mice at 5 and 30 min after olive oil gavage (n = 8 in each group). Data are presented as mean ± SEM. $*p < 0.05$. $**p < 0.01$. TM, tamoxifen.

expression was reduced by half in the gut mucosa of the *Ogt*-VKO mice (Figure 5B), and SGLT1 protein in the small intestine of the *Ogt*-VKO mice was approximately one-third of that of the control mice. (Figure 5C,D).

High intestinal inflammation causes malabsorption that may lead to low body weight and hypoglycaemia. To exclude this possibility, we examined the morphological changes and cytokine-related gene expression in the intestine. The *Ogt*-VKO mice showed no obvious inflammatory cell infiltration and no atrophy (SFigure 2A); they also showed no obvious increase of F4/80 positive macrophage infiltration in the small intestine upon histological analysis (SFigure 2B). Additionally, there was no obvious bloody stool or diarrhoea in the *Ogt*-VKO mice, which would suggest enteritis (SFigure 2C), and we did not observe shortening of the length of the intestine and the villus/crypt ratio in the *Ogt*-VKO mice, which would also indicate enteritis (SFigure 2D, E). Moreover, the *Tnf-α* and *F4/80* genes, which are involved in inflammation, were not enriched in the *Ogt*-VKO mice compared with the control mice, suggesting that gut inflammation is unlikely to be involved (SFigure 2F, G).

3.5. Inducible small intestine-specific depletion of OGT results in a decrease in body weight, glycaemia and intestinal sugar absorption

As demonstrated above, the *Ogt*-VKO mice were congenitally lacking *O*-GlcNAcylation in the intestine and presented underweight and lower glycaemia even at weaning. Therefore, to exclude the influence of growth during lactation, we generated tamoxifen-inducible intestinal epithelium-specific *Ogt*-knockout mice (*Ogt*-iVKO) (SFigure 3A). We observed suppressed intestinal *O*-GlcNAcylation in the *Ogt*-iVKO mice by immunostaining and western blotting with RL2 antibody (SFigure 3B, C). Before tamoxifen administration, the body weight and glycaemic levels were similar between the *Ogt*-iVKO and the control mice. However, body weight significantly reduced (24.5 ± 0.3 vs. 21.6 ± 0.3 g, $p < 0.05$) and blood glucose levels drastically decreased (7.0 ± 0.4 vs. 4.8 ± 0.4 mmol/l, $p < 0.05$) 2 weeks after tamoxifen treatment (Figure 6A,C). We measured ad libitum-fed plasma insulin levels in both the *Ogt*-iVKO and the control mice. *Ogt*-iVKO showed significantly lower plasma insulin compared with the control (204.6 ± 45.6 pM vs. 68.5 ± 14.4 pM, $p < 0.05$) (Figure 6B). The food intake of the *Ogt*-iVKO and the control mice after tamoxifen administration was similar (Figure 6D). Additionally, we observed significant weight loss even in pair feeding of the *Ogt*-iVKO mice (23.8 ± 0.8 vs. 20.5 ± 0.2 g, $p < 0.01$) (SFigure 4A).

In the *Ogt*-iVKO mice, the expression of SGLT1 protein was barely detected along the brush border of the small intestinal epithelium, with scarce *O*-GlcNAcylation assessed by RL2 antibody (SFigure 4B). Furthermore, *Sglt1* gene expression was significantly decreased, with strong suppression of *Ogt* gene expression ($p < 0.05$) in the *Ogt*-iVKO mice (SFigure 4C, D).

To elucidate that the intestinal glucose absorption was diminished in the *Ogt*-iVKO mice, we performed an oral D-xylose administration test in both the *Ogt*-iVKO and control mice. The D-xylose administration test is a functional test for intestional sugar absorption and has shown reflecting the SGLT1 facilitated glucose absorption ([21,22]). The *Ogt*-iVKO mice exhibited lower xylose levels at the early phase (30 min: 2.18 ± 0.13 mM vs. 1.54 ± 0.01 mM, $p < 0.05$) and AUC after oral administration (Figure 6E,F).

3.6. Glucose-dependent incretin secretion is inhibited in the *Ogt*-iVKO mice

Glucose stimulates GLP-1 and GIP release via SGLT1 from intestinal L cells or K cells; lipids are another stimulator of incretin secretion [24]. To examine whether loss of *O*-GlcNAcylation affects glucose-dependent incretin secretion through the reduced expression of SGLT1, we performed oral glucose and fat challenge tests and compared the incretin levels between the *Ogt*-iVKO and the control mice.

Oral glucose load (6 g/kg) raised glycaemia significantly less in the *Ogt*-iVKO mice than in the control mice (SFigure 5G). The *Ogt*-iVKO mice exhibited higher fasting GLP-1 levels (4.6 ± 0.8 vs. 9.3 ± 1.4 pmol/l, $p < 0.05$), whereas glucose-dependent GLP-1 secretion was notably suppressed (7.5 ± 0.9 vs. 4.1 ± 0.8 pmol/l, $p < 0.01$) at 5 and 30 min after glucose gavage (Figure 6G—I). Furthermore, glucose-dependent GIP secretion was suppressed at 5 min after glucose gavage, though the difference was not statistically significant (SFigure 5A—C). Contrary to the glucose-dependent incretin release, the *Ogt*-iVKO mice showed a significant increase in GIP secretion (SFigure 5D—F) and a slightly higher GLP-1 secretion (11.6 ± 2.2 vs. 16.7 ± 3.6 pmol/l; Figure 6J—L) at 30 min after olive oil gavage. These results suggest that *Ogt* depletion may be responsible for the decrease in glucose-induced incretin secretion.

Next, we counted cell numbers of K and L cells and measured *Gip* and *Gcg* (*proglucagon*) mRNA expression. The cell numbers of L cells and K cells were increased without significance in the *Ogt*-VKO mice (SFigure 6A, B), while in the *Ogt*-VKO mice, *Gcg* expression was slightly reduced, and *Gip* expression was significantly reduced (SFigure 7C, D).

3.7. *O*-GlcNAcylation regulates *Sglt1* gene expression

Enteroendocrine STC-1 cells secrete incretins in a glucose-dependent manner so we examined whether changes in *O*-GlcNAcylation affect the expression of *Sglt1* in STC-1 cells.

Glucosamine treatment, which increases *O*-GlcNAcylation, increased the expression of *O*-linked N-acetylglucosamine, which was detected with RL2 antibody, whereas OSMI1, an OGT inhibitor, totally diminished this expression (Figure 7A). Furthermore, glucosamine elevated and OSMI1 decreased *Sglt1* gene expression (Figure 7B). By contrast, the sugar transporter *Glut2* gene expression was not affected by these treatments. Moreover, *Glut5* gene expression was suppressed by OSMI1 treatment but not affected by glucosamine (Figure 7C,D). These results suggest that *O*-GlcNAcylation directly regulates *Sglt1* gene expression. Next, we investigated the interaction between *O*-GlcNAcylation and the cAMP-PKA pathway. *Sglt1* gene expression, which was elevated by glucosamine, was significantly reduced to the control level by treatment with H89, a PKA inhibitor (Figure 7E).

Additionally, in vivo, CREB phosphorylation, which is regulated by cAMP, was decreased in the intestinal epithelium of *Ogt*-VKO (Figure 7F,G). Furthermore, glucosamine significantly elevated CREB phosphorylation in STC-1 cells in vitro (Figure 7H,I). A CREB inhibitor, 666-15, reduced *Sglt1* expression in the glucosamine-treated STC-1 cells (Figure 7J).

To investigate whether other transcriptional factors are involved in *Sglt1* gene regulation, we analysed Sp-1 and HNF1 alpha expression. Sp-1 and HNF1 alpha protein expression inversely increased in the *Ogt*-VKO mice (SFigure 8C—E). By contrast, the nuclear localization of these transcriptional factors was comparable among the *Ogt*-VKO and the control mice (SFigure 8A, B).

3.8. Systemic knockdown of *O*-GlcNAcylation downregulates the expression of *Sglt1* in the intestine and the kidney

SGLT1 is robustly expressed in the epithelium of intestinal mucosa and in the proximal tubes of the kidney. Therefore, we generated mice with inducible systemic knockout of *Ogt* (*Ogt*-iKO) (SFigure 9A) and investigated whether *O*-GlcNAcylation regulates *Sglt1* expression, specifically in the small intestine.

In the systemic *Ogt*-iKO mice, we observed an extreme decrease in *O*-GlcNAcylation, which was assessed by the RL2 antibody (Figure 8A,D),

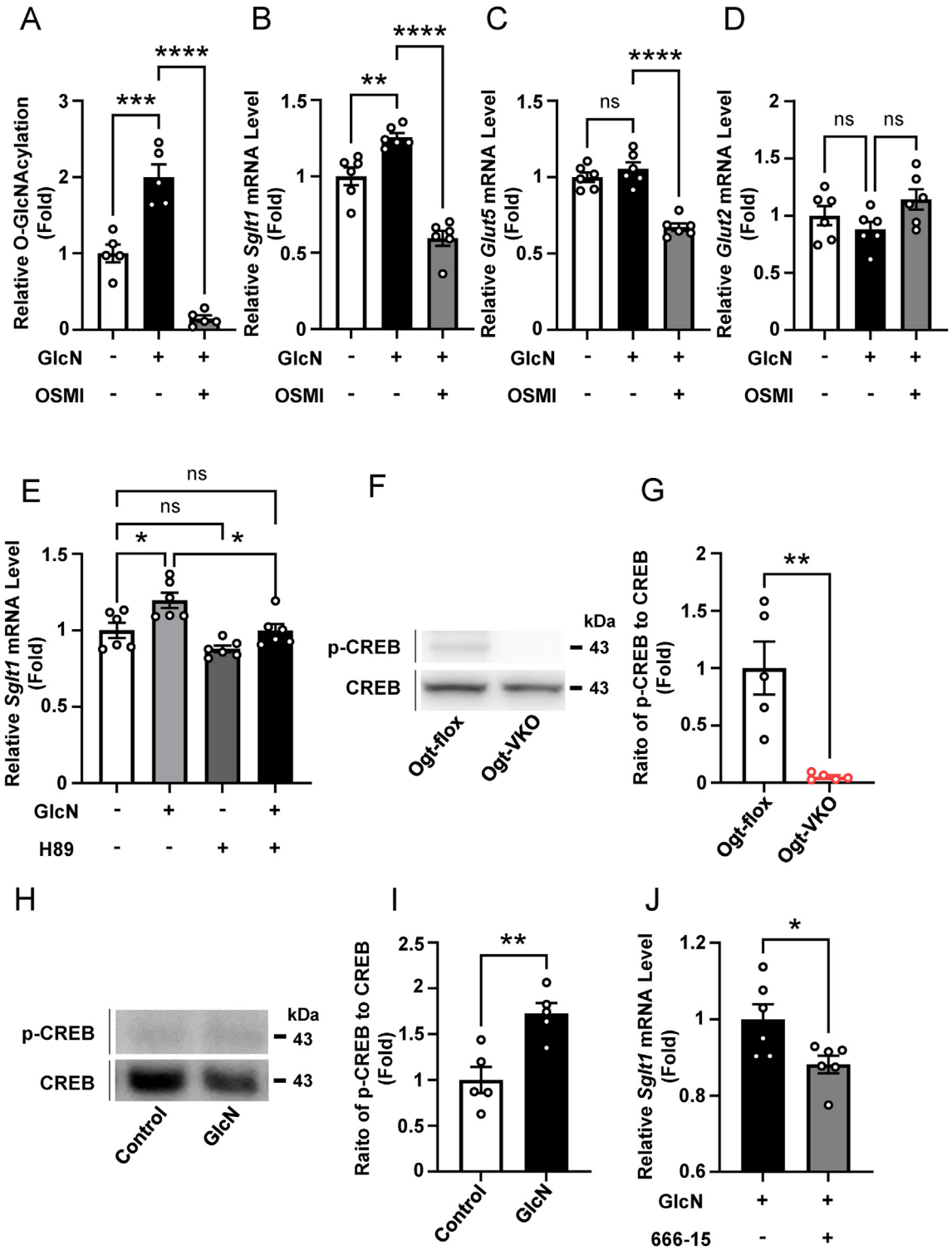

Figure 7: *O*-GlcNAcylation regulated *Sglt1* gene expression. (A) Quantification of western blot analysis of OGT and *O*-GlcNAcylation (RL2) in STC-1 cells (n = 5 in each group). Quantification of the gene expression of *Sglt1* (B), *Glut5* (C) and *Glut2* (D) in STC-1 cells (n = 6 in each group). (E) Quantification of gene expression of *Sglt1* by PKA inhibition in STC-1 cells (n = 6 in each group). (F) Representative western blot analysis of p-CREB and CREB levels in the intestinal epithelium of the *Ogt*-VKO and the control mice. (G) Quantitative ratio of p-CREB to CREB in the intestinal epithelium (n = 5 in each group). (H) Representative western blot analysis of p-CREB and CREB levels by glucosamine treatment in STC-1 cells. (I) Quantitative ratio of p-CREB to CREB by glucosamine treatment in STC-1 cells (n = 6 in each group). (J) Quantification of gene expression of *Sglt1* by CREB inhibition in glucosamine-treated STC-1 cells (n = 6 in each group). Data are presented as means ± SEM. $*p < 0.05$. GlcN, Glucosamine. OSMI, OSMI1.

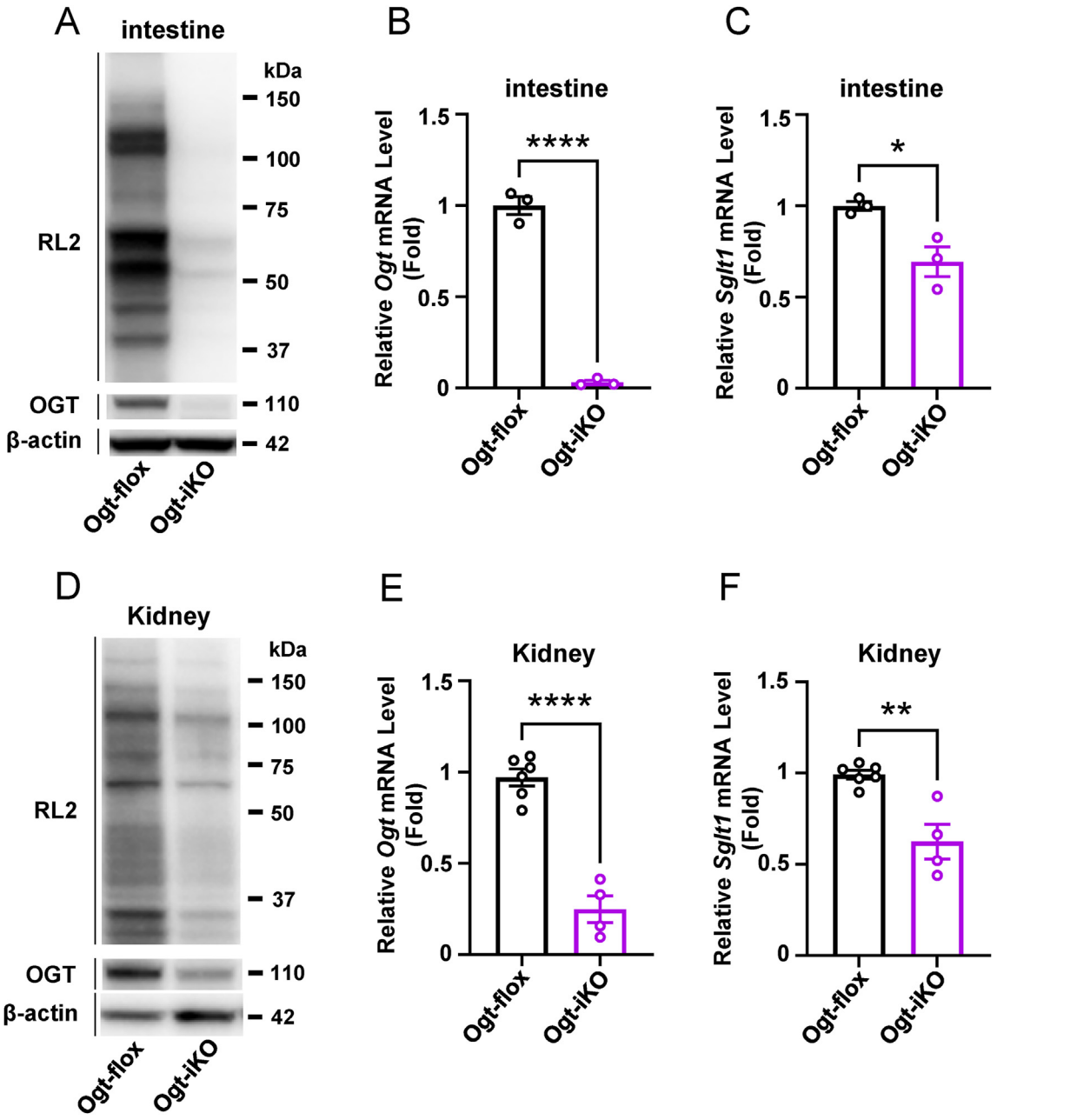

Figure 8: Systemic knockdown of *O*-GlcNAcylation downregulated the *Sglt1* expression in both the intestine and the kidney. (A) Representative western blot analysis of O-GlcNAcylation (RL2) and OGT in the intestinal epithelium. Quantification of the gene expression of *Ogt* (B) and *Sglt1* (C) in the intestinal epithelium (n = 3 in each group). (D) Representative western blot analysis of *O*-GlcNAcylation (RL2) and OGT in the kidney. Quantification of the gene expression of *Ogt* (E) and *Sglt1* (F) in the kidney (n = 6 in each group). Data are presented as means ± SEM. $^{*}p < 0.05$.

as well as a distinct downregulation of *Ogt* gene expression both in the small intestine and the kidney (Figure 8B,E). *Sglt1* expression was simultaneously suppressed in the small intestine and the kidney (Figure 8C,F), suggesting that *O*-GlcNAcylation modulated *Sglt1* expression in both organs.

4. DISCUSSION

In the current study, we first demonstrated that *O*-GlcNAcylation regulates glucose absorption through SGLT1 expression in the intestine. We extended our study to investigate how *O*-GlcNAcylation modulate protein and gene expression of SGLT1 both in *vivo* and in vitro.

The fasting mice showed that *O*-GlcNAcylation decreased in intestinal epithelial cells without changes in *Ogt* expression. The first step of *O*-GlcNAcylation is glucose entering the cell and incorporation into the hexosamine biosynthetic pathway. Therefore, we speculated that the reduction in glucose influx into the intestinal tract may result in the lack of substrate for *O*-GlcNAcylation, leading to the decrease in *O*-GlcNAcylation under fasting conditions. In rodents, fasting has been shown to decrease the gene expression of *Sglt1* in the intestine [25], but *SGLT1* gene expression has been reported to be increased by

dietary monosaccharide loading [26,27]. Therefore, we hypothesised that *O*-GlcNAcylation modifies the expression of *Sglt1* and regulates glucose absorption. We also postulated that the loss of the *O*-GlcNAcylation mimics the fasting metabolic condition in the intestine.

We therefore created intestinal epithelium-specific *Ogt*-VKO mice to further explore the roles of *O*-GlcNAcylation in the intestine. Indeed, the *Ogt*-VKO mice showed lower body weight and decreased glycaemia at any time from the time of weaning. It is possible that the changes in body weight and glycaemia in the *Ogt*-VKO mice after weaning may have already been determined at weaning. Nevertheless, we cannot exclude the possibility that the cachexia-like phenotype of the *Ogt*-VKO mice contributed to the improved glucose tolerance that we observed. Thus, we generated the *Ogt*-iVKO mice, which are tamoxifen-inducible intestinal epithelium-specific *Ogt*-deficient mice. We showed that the suppression of *O*-GlcNAcylation in the intestine markedly reduced body weight and blood glucose levels only after tamoxifen administration. There was no difference in food intake between the *Ogt*-iVKO and the control mice, and the *Ogt*-iVKO mice showed significant weight loss even after pair feeding. Thus, it is unlikely that the decrease in food intake due to appetite suppression caused the weight loss and lower glycaemia.

We then examined whether glucose absorption was affected by the loss of *O*-GlcNAcylation. Our results suggest that the decreased SGLT1 expression may be the cause of the decreased glucose absorption in the *Ogt*-VKO mice. We have consistently shown, in previous work, that postprandial hyperglycaemia was linked to increased glucose absorption via enhanced SGLT1 expression in spontaneous diabetic rats at the early step of glucose intolerance [22]. To directly access the intestinal glucose absorption, we performed a D-xylose administration test in the *Ogt*-iVKO mice, which is clinically used for the diagnosis of sugar malabsorption from the gut. A putative SGLT1/2 inhibitor, phlorizin, blocks D-xylose absorption [22]. As postulated, the *Ogt*-iVKO mice exhibited lower peak levels and AUC after the oral D-xylose administration, suggesting that the *Ogt*-iVKO mice presented limited glucose absorption with a decrease in the intestinal SGLT1 expression. The *Ogt*-VKO mice on the other hand showed a higher peak triglyceride level than the control mice did in the OOTT. There are two possible reasons why: (1) enhanced lipid absorption from the intestine and (2) delayed triglyceride metabolism in the body. In the *Ogt*-VKO mice, triglycerides disappeared significantly faster when given via i.v. injection. Therefore, the increase in triglycerides after the oral OOTT in the *Ogt*-VKO mice is likely due to an increase in triglyceride absorption rather than a decrease in triglyceride metabolism.

Additionally, the faecal lipid contents from the *Ogt*-VKO mice significantly decreased and the RQ significantly decreased from the dawn to the early light period compared with the control mice. These results suggest that the *Ogt*-VKO mice might switch to utilize more lipid than glucose for energy sources. By contrast, the RQ was elevated from the late light phase without fluctuation in locomotive activities in the *Ogt*-VKO mice. We considered that the *Ogt*-VKO mice retained energy by constant food consumption, lower activity in the late dark phase and consistent lower energy expenditure—resulting in behavioural changes—because their carbohydrate absorption from the intestine was diminished. Also, the body-weight comparable *Ogt*-iVKO mice just after their tamoxifen induction showed similar metabolic changes to the *Ogt*-VKO mice (SFigure 7A—G, I). Moreover, our data indicated that average EE values were not correlated with respective body weight (Figure 4H, SFigure 7H), suggesting that the genetic manipulation was the driving differences in EE. Therefore, we speculate that it is not being underweight but a lack of *O*-GlcNAcylation in the intestine that can contribute to those metabolic changes.

A previous report indicated that decreased *O*-GlcNAcylation in the intestine induced inflammation in the lower small intestine and colon [28] and was often accompanied by nutritional malabsorption. However, our study showed that the *Ogt*-VKO mice did not present severe inflammation in the upper small intestine at the time of our experiments. We presume that this discrepancy may be because we focused on a different part of the small intestine. The gut bacterial flora is related to enteritis or gut inflammation. As reported previously, a mouse model of the inflammatory bowel disease exhibited different susceptibility of T cell-induced colitis by relocation of the experimental facilities [29]. It is also possible that environmental factors influence the gut bacterial flora, resulting in the different results. In our preliminary study, older (approximately 20-week-old) *Ogt*-VKO mice indeed tended to show the shortening of villus length, which may be related to enteritis. However, we consider this intestinal change as secondary to non-absorbed glucose retention in the intestine by diminished SGLT1 expression, as reported in SGLT1-deficient human and mice subjects [8,30].

SGLT1 is involved in glucose absorption by the intestinal absorptive epithelial cells, and it regulates glucose-dependent incretin secretion from enteroendocrine cells such as GLP-1-secreting L cells and GIP-secreting K cells [10]. In the *Ogt*-VKO mice, incretin secretion was increased during fasting, as previously shown [31]. By contrast, glucose-dependent GLP-1 secretion was significantly suppressed in the *Ogt*-VKO mice, similarly to the *Sglt1*-knockout mice. Incretin secretion is regulated not only by glucose but also by lipid absorption. In our study, oil-dependent GLP-1 secretion was intact and tended to increase after oral olive oil loading, similarly to the *Sglt1*-knockout mice [10]. The number of L cells showed a slight increase, without significance, while *Gcg* expression showed a slight decrease; thus, we consider that fasting GLP-1 secretion might be higher due to the increased L cell number in the intestine as previously reported.

The Sglt1-knockout mice exhibited lower glucose-induced GIP secretion but comparable oil-induced GIP secretion to the wild-type mice [10], while the *Ogt*-iVKO mice exhibited similar glucose-induced GIP secretion but enhanced oil-induced GIP secretion compared with the control. It was previously shown that glucose-induced GIP secretion in non-diabetic states is mainly dependent on SGLT1, whereas in the diabetic state, SGLT1 as well as KATP channels are involved in GIP secretion [21]. We assume that compensatory mechanisms such as enhanced KATP channel-dependent pathway might be involved in the lack of change in glucose-induced GIP secretion in the *Ogt*-VKO mice.

Next, we confirmed that *O*-GlcNAcylation directly induced *Sglt1* gene expression in STC-1 cells. One possible mechanism is that *O*-GlcNAcylation is directly related to the mRNA stability of *Sglt1*. Previous reports have shown that the cAMP-induced expression of human antigen R (HuR) is involved in stabilisation of *SGLT1* mRNA [32,33]. Indeed, H89, a PKA inhibitor, diminished the *Sglt1* gene expression, which was increased by activated *O*-GlcNAcylation in STC-1 cells. We speculated that *O*-GlcNAcylation partly regulated the stability of *Sglt1* mRNA through cAMP. Another possible mechanism is that *O*-GlcNAcylation regulates *Sglt1* transcription. Earlier research demonstrated that inhibition of CREB signalling by a compound reduced *SGLT1* gene expression in vivo and in vitro [34], and another previous study demonstrated that downregulation of *O*-GlcNAcylation caused decreases in the phosphorylation of CREB at Ser133 [35]. Our study showed that phosphorylation of CREB was markedly reduced in the *Ogt*-VKO mice, suggesting that *O*-GlcNAcylation might regulate *Sglt1* transcription through the cAMP-CREB pathway. Other than CREB, we observed the expression of Sp-1 and HNF1 alpha, which were known

to increase *Sglt1* transcription [36,37] and to be *O*-GlcNAcylated [38,39]. Sp-1 and HNF1 alpha protein expression inversely increased in the *Ogt*-VKO mice. By contrast, the nuclear localization of these transcriptional factors was comparable among the *Ogt*-VKO and the control, so we consider that these transcriptional factors did not contribute to *Sglt1* downregulation in the *Ogt*-VKO mice.

SGLT1 is predominantly expressed in the intestine, but it is also expressed in the proximal tubules of the kidney, where it is involved in glucose reabsorption. Our results showed that both *O*-GlcNAcylation and *Sglt1* gene expression were decreased in the kidney as well as in intestinal epithelial cells, suggesting that *O*-GlcNAcylation is crucial and regulates *Sglt1* gene expression in a manner that is not tissue specific.

The current study has several limitations. First, we did not demonstrate the relevance of intestinal *O*-GlcNAcylation to metabolic disorders such as obesity and diabetes. Previous studies have indicated that sugar absorption is boosted through the increment of SGLT1 expression in diabetes which aggravates hyperglycaemia [13–17]. Second, we did not elucidate how lipid absorption and metabolism were enhanced to compensate for the decreased glucose absorption in the *Ogt*-VKO mice. Third, we did not identify the *O*-GlcNAcylated protein(s) involved and how these proteins regulate the *SGLT1* gene expression. Additional studies are required to elucidate the mechanisms involved in the direct relationship between *O*-GlcNAcylation and *SGLT1* gene regulation.

Collectively, suppression of *O*-GlcNAcylation in the intestine reduced glucose absorption and inhibited SGLT1 expression. Controlling *O*-GlcNAcylation in the intestine may lead to new treatments for absorption disorders, obesity and diabetes.

DATA AVAILABILITY

The data that support the findings of this study are available from the corresponding author upon reasonable request.

FUNDING

This study was supported by Grants-in-Aid for Scientific Research (KAKENHI) from the Japan Society for the Promotion of Science (H.M. 18H02862, S.U. 19K08998). The study was funded by the Shiga University of Medical Science.

This study was also supported by research promotion grants from Nipro, Bayer Yakuhin, Boehringer-Ingelheim, Kyowa Hakko Kirin, Kowa Pharmaceuticals, Sumitomo Dainippon Pharma Co., Ltd., Daiichi-Sankyo, Takeda Pharmaceutical Company Limited, Novo Nordisk Pharma, Mitsubishi Tanabe, Sanwa Kagaku Kenkyusho, MSD and Mochida Pharmaceutical Co., Ltd.

CONTRIBUTION STATEMENT

K Nishimura, YF, SI, TY, NO, SU and HM designed the study. K Nishimura, YF, SI, TY, NO, K Nishi and YI conducted the research. K Nishimura, YF, SI, TY, K Nishi, SU, KM and SU analysed and interpreted the data. K Nishimura, YF and HM wrote the manuscript. K Nishimura, YF, SI, TY, NO, K Nishi, AN, YI, KM, SU, EN, AA and HM reviewed and edited the manuscript. YF had primary responsibility for the final content. All authors read and approved the final manuscript.

CONFLICT OF INTEREST

The authors declare that there is no duality of interest associated with this manuscript.

ACKNOWLEDGEMENTS

We are indebted to Dr. Itsuko Miyazawa, Miss Keiko Kosaka, Dr. Takayuki Imai, Dr. Miwako Katagi, Miss Yuki Nakae and the Central Research Laboratory of Shiga University of Medical Science for their expert technical assistances in this study. The authors thank Dr. Sylvie Robine (Institut Curie, France) and Dr. Wakana Ohashi (Keio University, Japan) for providing the Vil-CreERT2 mice. We thank Michal Bell, PhD, from Edanz (https://jp.edanz.com/ac) for editing a draft of this manuscript. We acknowledge Dr. Scott Covey and Professor Timothy J. Kieffer (University of British Columbia, Canada) for crucial discussions and insightful suggestions.

APPENDIX A. SUPPLEMENTARY DATA

Supplementary data to this article can be found online at https://doi.org/10.1016/j.molmet.2022.101458.

REFERENCES

[1] van der Flier, L.G., Clevers, H., 2009. Stem cells, self-renewal, and differentiation in the intestinal epithelium. Annual Review of Physiology 71:241–260.

[2] Goodman, B.E., 2010. Insights into digestion and absorption of major nutrients in humans. Advances in Physiology Education 34(2):44–53.

[3] Drucker, D.J., 2006. The biology of incretin hormones. Cell Metabolism 3(3):153–165.

[4] Cho, Y.M., Fujita, Y., Kieffer, T.J., 2014. Glucagon-like peptide-1: glucose homeostasis and beyond. Annual Review of Physiology 76:535–559.

[5] DeFronzo, R.A., Eldor, R., Abdul-Ghani, M., 2013. Pathophysiologic approach to therapy in patients with newly diagnosed type 2 diabetes. Diabetes Care 36(Suppl. 2):S127–S138.

[6] DeFronzo, R.A., 2017. Combination therapy with GLP-1 receptor agonist and SGLT2 inhibitor. Diabetes, Obesity and Metabolism 19(10):1353–1362.

[7] Koepsell, H., 2020. Glucose transporters in the small intestine in health and disease. Pflügers Archiv 472(9):1207–1248.

[8] Martín, M.G., Turk, E., Lostao, M.P., Kerner, C., Wright, E.M., 1996. Defects in Na+/glucose cotransporter (SGLT1) trafficking and function cause glucose-galactose malabsorption. Nature Genetics 12(2):216–220.

[9] Wright, E.M., Turk, E., Martin, M.G., 2002. Molecular basis for glucose-galactose malabsorption. Cell Biochemistry and Biophysics 36(2–3):115–121.

[10] Gorboulev, V., Schürmann, A., Vallon, V., Kipp, H., Jaschke, A., Klessen, D., et al., 2012. Na(+)-D-glucose cotransporter SGLT1 is pivotal for intestinal glucose absorption and glucose-dependent incretin secretion. Diabetes 61(1):187–196.

[11] Yang, X., Qian, K., 2017. Protein O-GlcNAcylation: emerging mechanisms and functions. Nature Reviews Molecular Cell Biology 18(7):452–465.

[12] Ruan, H.B., Singh, J.P., Li, M.D., Wu, J., Yang, X., 2013. Cracking the O-GlcNAc code in metabolism. Trends in Endocrinology & Metabolism 24(6):301–309.

[13] Ma, J., Hart, G.W., 2013. Protein O-GlcNAcylation in diabetes and diabetic complications. Expert Review of Proteomics 10(4):365–380.

[14] Issad, T., Kuo, M., 2008. O-GlcNAc modification of transcription factors, glucose sensing and glucotoxicity. Trends in Endocrinology & Metabolism 19(10):380–389.

[15] Cox, E.J., Marsh, S.A., 2013. Exercise and diabetes have opposite effects on the assembly and O-GlcNAc modification of the mSin3A/HDAC1/2 complex in the heart. Cardiovascular Diabetology 12:101.

[16] Wang, X., Feng, Z., Yang, L., Han, S., Cao, K., Xu, J., et al., 2016. O-GlcNAcase deficiency suppresses skeletal myogenesis and insulin sensitivity in mice through the modulation of mitochondrial homeostasis. Diabetologia 59(6):1287–1296.

[17] Masaki, N., Feng, B., Bretón-Romero, R., Inagaki, E., Weisbrod, R.M., Fetterman, J.L., et al., 2020. O-GlcNAcylation mediates glucose-induced alterations in endothelial cell phenotype in human diabetes mellitus. Journal of American Heart Association 9(12):e014046.

[18] Ida, S., Morino, K., Sekine, O., Ohashi, N., Kume, S., Chano, T., et al., 2017. Diverse metabolic effects of O-GlcNAcylation in the pancreas but limited effects in insulin-sensitive organs in mice. Diabetologia 60(9):1761—1769.

[19] Weinstein, M.M., Yin, L., Beigneux, A.P., Davies, B.S., Gin, P., Estrada, K., et al., 2008. Abnormal patterns of lipoprotein lipase release into the plasma in GPIHBP1-deficient mice. Journal of Biological Chemistry 283(50):34511—34518.

[20] Bligh, E.G., Dyer, W.J., 1959. A rapid method of total lipid extraction and purification. Canadian Journal of Biochemistry and Physiology 37(8):911—917.

[21] Ogata, H., Seino, Y., Harada, N., Iida, A., Suzuki, K., Izumoto, T., et al., 2014. KATP channel as well as SGLT1 participates in GIP secretion in the diabetic state. Journal of Endocrinology 222(2):191—200.

[22] Fujita, Y., Kojima, H., Hidaka, H., Fujimiya, M., Kashiwagi, A., Kikkawa, R., 1998. Increased intestinal glucose absorption and postprandial hyperglycaemia at the early step of glucose intolerance in Otsuka Long-Evans Tokushima Fatty rats. Diabetologia 41(12):1459—1466.

[23] Hart, G.W., 2019. Nutrient regulation of signaling and transcription. Journal of Biological Chemistry 294(7):2211—2231.

[24] Ezcurra, M., Reimann, F., Gribble, F.M., Emery, E., 2013. Molecular mechanisms of incretin hormone secretion. Current Opinion in Pharmacology 13(6):922—927.

[25] Honma, K., Masuda, Y., Mochizuki, K., Goda, T., 2014. Re-feeding rats a high-sucrose diet after 3 days of starvation enhances histone H3 acetylation in transcribed region and expression of jejunal GLUT5 gene. Bioscience Biotechnology & Biochemistry 78(6):1071—1073.

[26] Miyamoto, K., Hase, K., Takagi, T., Fujii, T., Taketani, Y., Minami, H., et al., 1993. Differential responses of intestinal glucose transporter mRNA transcripts to levels of dietary sugars. Biochemical Journal 295(Pt 1):211—215.

[27] Kishi, K., Tanaka, T., Igawa, M., Takase, S., Goda, T., 1999. Sucrase-isomaltase and hexose transporter gene expressions are coordinately enhanced by dietary fructose in rat jejunum. Journal of Nutrition 129(5):953—956.

[28] Zhao, M., Xiong, X., Ren, K., Xu, B., Cheng, M., Sahu, C., et al., 2018. Deficiency in intestinal epithelial O-GlcNAcylation predisposes to gut inflammation. EMBO Molecular Medicine 10(8).

[29] Reinoso Webb, C., den Bakker, H., Koboziev, I., Jones-Hall, Y., Rao Kottapalli, K., Ostanin, D., et al., 2018. Differential susceptibility to T cell-induced colitis in mice: role of the intestinal microbiota. Inflammatory Bowel Diseases 24(2):361—379.

[30] Powell, D.R., Smith, M.G., Doree, D.D., Harris, A.L., Greer, J., DaCosta, C.M., et al., 2017. LX2761, a sodium/glucose cotransporter 1 inhibitor restricted to the intestine, improves glycemic control in mice. Journal of Pharmacology and Experimental Therapeutics 362(1):85—97.

[31] Zhao, M., Ren, K., Xiong, X., Cheng, M., Zhang, Z., Huang, Z., et al., 2020. Protein O-GlcNAc modification links dietary and gut microbial cues to the differentiation of enteroendocrine L cells. Cell Reports 32(6):108013.

[32] Loflin, P., Lever, J.E., 2001. HuR binds a cyclic nucleotide-dependent, stabilizing domain in the 3′ untranslated region of Na(+)/glucose cotransporter (SGLT1) mRNA. FEBS Letters 509(2):267—271.

[33] Lee, W.Y., Loflin, P., Clancey, C.J., Peng, H., Lever, J.E., 2000. Cyclic nucleotide regulation of Na+/glucose cotransporter (SGLT1) mRNA stability. Interaction of a nucleocytoplasmic protein with a regulatory domain in the 3′-untranslated region critical for stabilization. Journal of Biological Chemistry 275(43):33998—34008.

[34] Wang, C.W., Su, S.C., Huang, S.F., Huang, Y.C., Chan, F.N., Kuo, Y.H., et al., 2015. An essential role of cAMP response element binding protein in ginsenoside Rg1-mediated inhibition of Na+/glucose cotransporter 1 gene expression. Molecular Pharmacology 88(6):1072—1083.

[35] Xie, S., Jin, N., Gu, J., Shi, J., Sun, J., Chu, D., et al., 2016. O-GlcNAcylation of protein kinase A catalytic subunits enhances its activity: a mechanism linked to learning and memory deficits in Alzheimer's disease. Aging Cell 15(3):455—464.

[36] Martín, M.G., Wang, J., Solorzano-Vargas, R.S., Lam, J.T., Turk, E., Wright, E.M., 2000. Regulation of the human Na(+)-glucose cotransporter gene, SGLT1, by HNF-1 and Sp1. American Journal of Physiology — Gastrointestinal and Liver Physiology 278(4):G591—G603.

[37] Vayro, S., Wood, I.S., Dyer, J., Shirazi-Beechey, S.P., 2001. Transcriptional regulation of the ovine intestinal Na+/glucose cotransporter SGLT1 gene. Role of HNF-1 in glucose activation of promoter function. European Journal of Biochemistry 268(20):5460—5470.

[38] Suh, H.N., Lee, Y.J., Kim, M.O., Ryu, J.M., Han, H.J., 2014. Glucosamine-induced Sp1 O-GlcNAcylation ameliorates hypoxia-induced SGLT dysfunction in primary cultured renal proximal tubule cells. Journal of Cellular Physiology 229(10):1557—1568.

[39] Zhang, C., Xie, F., Li, L., Zhang, Y., Ying, W., Liu, L., et al., 2019. Hepatocyte nuclear factor 1 alpha (HNF1A) regulates transcription of O-GlcNAc transferase in a negative feedback mechanism. FEBS Letters 593(10):1050—1060.

